RSC Advances

PAPER

View Article Online
View Journal | View Issue

Cite this: *RSC Adv.*, 2017, **7**, 48394

Tri- and hexanuclear heterometallic Ni(II)–M(II) (M = Ca, Sr and Ba) bis(salamo)-type complexes: synthesis, structure and fluorescence properties†

Xiu-Yan Dong,[a] Xiao-Yan Li,[a] Ling-Zhi Liu,[a] Han Zhang,[a] Yu-Jie Ding[b] and Wen-Kui Dong *[a]

Received 16th July 2017
Accepted 10th October 2017

DOI: 10.1039/c7ra07826a

rsc.li/rsc-advances

Three heterometallic Ni(II)–M(II) (M = Ca, Sr and Ba) complexes, two discrete heterotrinuclear complexes $[Ni_2(L)Ca(OAc)_2(CH_3OH)_2]\cdot 2C_2H_5OH\cdot 2CHCl_3$ (**1**) and $[Ni_2(L)Sr(OAc)_2(CH_3OH)_2]\cdot 2CH_3OH\cdot 2CH_2Cl_2$ (**2**) and a discrete heterohexanuclear dimer $[Ni_2(L)Ba(OAc)_2(CH_3OH)_2(H_2O)]_2\cdot 2CH_3OH$ (**3**), were synthesized with a naphthalenediol-based acyclic bis(salamo)-type ligand (H_4L), and characterized by elemental analyses, IR, UV-vis spectra, fluorescence spectra and X-ray crystallography. The heterometallic complexes were acquired by the reaction of H_4L with 2 equiv. of $Ni(OAc)_2\cdot 4H_2O$ and 1 equiv. of $M(OAc)_2$ (M = Ca, Sr and Ba). The crystal structures of complexes **1–3** have been determined by single-crystal X-ray diffractions. Owing to the different nature of the N_2O_2 and O_6 sites of the ligand H_4L, the introduction of two different metal(II) atoms to the site-selective moiety, leads to the two Ni(II) atoms occupied both the N_2O_2 sites, an alkaline earth metal atom occupied the O_6 site of the ligand $(L)^{4-}$ unit, respectively. Furthermore, the fluorescence properties have been discussed.

Introduction

The condensation between an aldehyde and an amine leading to a salamo-type bisoxime was first described by Nabeshima's group.[1] Structurally, salen-type ligands[2] are nitrogen analogue of an aldehyde or ketone in which the carbonyl group (CO) has been replaced by an imine or azomethine group. The properties of salen-type ligands may be easily altered and as such they are able to coordinate metals in a highly versatile way and combine with O-donors to provide multidentate ligand systems.[3] Salen-type N_2O_2 metal complexes are used as precursors to synthesize the oligometallic complexes owing to the high coordination ability of the phenoxo groups which can bridge two metal centers in a μ_2-M–O–M fashion.[4] Then, such μ_2-phenoxo bridging is also particularly important for the d-block homo- and heterometallic complexes of salen-type ligands, some of which exhibit interesting catalysis,[5] sensors,[6] electrochemical,[7] luminescence[8] and magnetism.[9] In recent years, our group has focused on the conversion of an acyclic molecule (bis(salamo)-type ligand) to the corresponding cyclic metal host, which can afford a larger C-shaped O_6 site on the metalation of the N_2O_2 sites and effectively control the guest recognition.[10] Thus, the O_6 site of this type of ligands are particularly suitable for the larger radius of the alkaline earth and rare earth metals to afford 3d–2s and 3d–4f heterometallic complexes exhibiting better crystal structures and photochemical properties.

Herein, as an extension of our previous studies,[10] a new acyclic bis(salamo)-type ligand H_4L is synthesized, in which two N_2O_2 salamo moieties share one naphthalenediol. As sizes of N_2O_2 and O_6 cavities are different, it is possible to synthesize the heterometallic complexes.[11,12] In this paper, heterometallic complexes $[Ni_2(L)Ca(OAc)_2(CH_3OH)_2]\cdot 2C_2H_5OH\cdot 2CHCl_3$ (**1**) $[Ni_2(L)Sr(OAc)_2(CH_3OH)_2]\cdot 2CH_3OH\cdot 2CH_2Cl_2$ (**2**) and $[Ni_2(L)Ba(OAc)_2(CH_3OH)_2(H_2O)]_2\cdot 2CH_3OH$ (**3**) have been synthesized and structurally characterized. In complex **2**, two μ_2-acetate ions bridge Ni(II) and Sr(II) atoms in a common μ_2-fashion, another μ_2-acetate ion chelates Sr(II) atom as a bidentate ligand. In complex **3**, two μ_2-acetate ions bridge the Ba1 and $Ba1^{\#2}$ atoms in a familiar μ_2-fashion, finally forming a hetero-hexanuclear dimer. To our knowledge, this novel 2 : 6 ($(L)^{4-}$: M^{2+}) hetero-hexanuclear complex isn't reported in the bis(salamo)-type complexes.[1,2e,11c]

Experimental

Materials and general methods

2-Hydroxy-3-methoxybenzaldehyde (99%), methyl trioctyl ammonium chloride (90%), pyridiniumchlorochromate (98%) and borontribromide (99.9%) were purchased from Alfa Aesar. Hydrobromic acid 33 wt% solution in acetic acid was purchased

[a]School of Chemical and Biological Engineering, Lanzhou Jiaotong University, Lanzhou, Gansu 730070, PR China. E-mail: dongwk@126.com

[b]School of Biological & Chemical Engineering, Anhui Polytechnic University, Wuhu 241000, PR China

† Electronic supplementary information (ESI) available. CCDC 1562392–1562394. For ESI and crystallographic data in CIF or other electronic format see DOI: 10.1039/c7ra07826a

from J&K Scientific Ltd. The other reagents and solvents were purchased from Shanghai Darui Chemical Fine Chemicals Company. Elemental analyses were performed by using a GmbH Vario EL V3.00 automatic elemental analysis instrument. Elemental analyses for metals were detected with an IRIS ER/S-WP-1 ICP atomic emission spectrometer. FT-IR spectra were recorded on a VERTEX70 FT-IR spectrophotometer, with samples prepared as KBr (400–4000 cm^{-1}) pellets. UV-vis absorption spectra were recorded on a Hitachi U-3900H spectrometer. ^{1}H and ^{13}C NMR spectra were determined by German Bruker AVANCE DRX-400 spectrometer. Fluorescent spectra were taken on a LS-55 fluorescence photometer. X-ray single crystal structure determinations were carried out on a SuperNova, Dual, Cu at zero, Eos four-circle diffractometer. FTICR-MS spectra were obtained on a Bruker Daltonics APEX-II 47e spectrometer. Melting points were obtained with the use of an X4 microscopic melting point apparatus made by the Beijing Taike Instrument Limited Company and were uncorrected.

Synthesis of the ligand H_4L

The reaction steps involved in the synthesis of the bis(salamo)-type tetraoxime ligand (H_4L) are shown in Scheme 1. 2,3-Dihydroxynaphthalene-1,4-dicarbaldehyde was prepared according to a literature procedure;[13] 1,2-bis(aminooxy)ethane[14] and 2-[*O*-(1-ethyloxyamide)]oxime-6-methoxyphenol[15] were synthesized according to an analogous method.

A solution of 2,3-dihydroxynaphthalene-1,4-dicarbaldehyde (432.08 mg, 2 mmol) in ethanol (20 mL) was added dropwise to a solution of 2-[*O*-(1-ethyloxyamide)]oxime-6-methoxyphenol (904.4 mg, 4 mmol) in ethanol (20 mL) under room temperature, the mixture was heated to reflux and kept refluxing for 6 h. Then cooled down to room temperature and the yellow precipitates were filtered and washed successively with ethanol and *n*-hexane, respectively. Several light yellow powdery solid (H_4L) were obtained and collected by filtration, washed with absolute ethanol and dried under vacuum. Yield: 712.63 mg, 56.36%; mp: 172 °C; ^{1}H NMR ($CDCl_3$, 400 MHz) δ 11.03 (s, 2H, OH), 9.82 (s, 2H, OH), 9.14 (s, 2H, CH=N), 8.29 (s, 2H, CH=N), 7.97 (q, J = 3.2 Hz, 2H, ArH), 7.41 (q, J = 6.0, 2.9 Hz, 2H, ArH), 7.06–6.68 (m, 6H, ArH), 4.58 (t, 8H, CH_2), 3.89 (s, 6H, CH_3) (Fig. S1†). ^{13}C NMR (DMSO, 151 MHz) δ 148.4 (s), 148.2 (s), 147.3 (s), 147.2 (s), 146.1 (s), 126.2 (s), 125.4 (s), 123.9 (s), 119.7 (s), 119.0 (s), 118.4 (s), 113.7 (s), 111.4 (s), 73.0 (s), 72.8 (s), 56.3 (s)

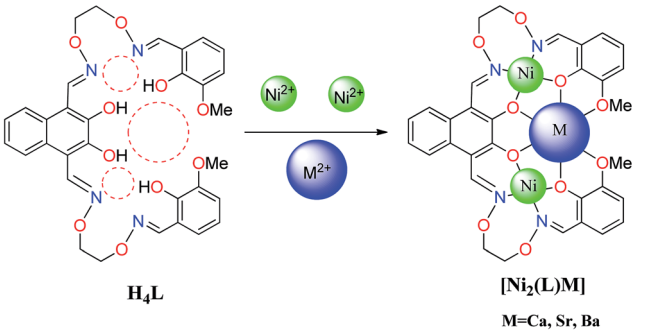

Scheme 2 Synthesis of heterometallic Ni(II)–M(II) complexes **1–3**.

(Fig. S2†). HRMS *m*/*z*: calc. for $C_{32}H_{32}N_4O_{10}Na$: $[H_4L + Na]^+$ 655.20, found: 655.2011 (Fig. S3†). Elemental analysis: anal. calc. for $C_{32}H_{32}N_4O_{10}$: C, 60.75; H, 5.10; N, 8.86, found (%): C, 60.38; H, 5.38; N, 8.65. IR (KBr; cm^{-1}): 1604 [ν(C=N)], 1248 [ν(Ar–O)], 3172 [ν(O–H)]. UV-vis [in methanol/dichloromethane (1 : 1)], λ_{max} (nm) [2.5 × 10^{-5} M]: 267, 341, 356, 376.

Preparation of complexes 1–3

Heterometallic complexes were synthesized by the reaction of H_4L with $Ni(OAc)_2\cdot 4H_2O$ and $M(OAc)_2$ (M(II) = Ca, Sr and Ba) (Scheme 2).

A solution of $Ni(OAc)_2\cdot 4H_2O$ (9.96 mg, 0.040 mmol) in ethanol (2 mL) and $Ca(OAc)_2$ (3.16 mg, 0.020 mmol) in water/methanol (1 : 3, 2 mL) were added to a solution of H_4L (12.64 mg, 0.020 mmol) in chloroform (4 mL), and the resulting solution was evaporated to dryness, after which the residue was added to dichloromethane/methanol (1 : 1, 8 mL) and heated to dissolve it and then cooled in the refrigerator and recrystallized. The color of the mixed solution turned dark green. The mixture was filtered and the filtrate was allowed to stand at room temperature for approximately three weeks. The solvent was partially evaporated and several clear dark green prismatic single crystals of complex **1** were obtained.

A solution of $Ni(OAc)_2\cdot 4H_2O$ (9.96 mg, 0.040 mmol) in methanol (2 mL) and $Sr(OAc)_2$ (3.16 mg, 0.020 mmol) in water/methanol (1 : 3, 2 mL) were added to a solution of H_4L (12.64 mg, 0.020 mmol) in dichloromethane (4 mL). The next steps are similar to complex **1**. Complex **3** was prepared by a similar procedure as for complex **2**.

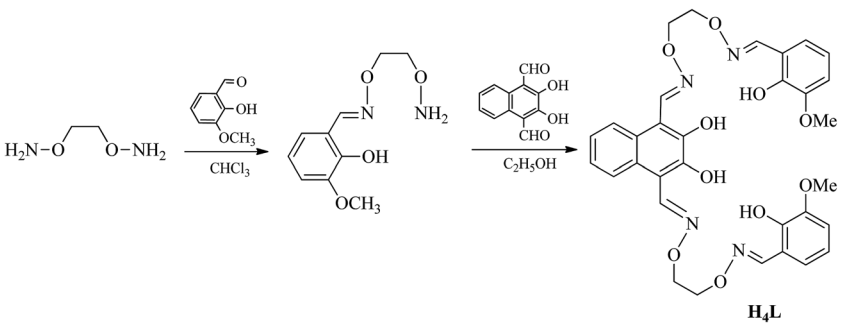

Scheme 1 Synthetic route to the bis(salamo)-type tetraoxime ligand H_4L.

Table 1 Crystallographic data and refinement parameters for complexes **1**, **2** and **3**

Complex	**1**	**2**	**3**
Formula	$C_{44}H_{56}Cl_6CaN_4O_{18}Ni_2$	$C_{42}H_{54}Cl_4SrN_4O_{18}Ni_2$	$C_{78}H_{96}Ba_2N_8O_{36}Ni_4$
Formula weight	1299.12	1247.99	2230.14
T (K)	291(2)	155(10)	294(14)
Radiation (Å)	Mo Kα, 0.71073	Mo Kα, 0.71073	Mo Kα, 0.71073
Crystal system	Monoclinic	Orthorhombic	Monoclinic
Space group	$P2_1/n$	$Pbcn$	$P2_1/n$
a (Å)	15.4086(8)	23.6620(5)	15.8005(3)
b (Å)	12.0628(6)	17.8187(5)	15.7041(3)
c (Å)	29.5294(9)	12.4666(3)	18.2762(4)
α (°)	90	90	90
β (°)	100.627(5)	90	94.551(19)
γ (°)	90	90	90
Volume (Å^3)	5394.5(4)	5256.2(2)	4520.62(16)
Z	4	4	4
D_c (g cm^{-3})	1.600	1.579	1.639
Absorption coefficient (mm^{-1})	1.164	1.996	1.764
Θ range for data collection(°)	1.397 to 25.997	3.862 to 24.112	3.510 to 27.218
F (000)	2680	2560.0	2264.0
Index ranges	$-19 \le h \le 13$, $-14 \le k \le 13$, $-36 \le l \le 35$,	$-23 \le h \le 29$, $-21 \le k \le 21$ $-15 \le l \le 15$,	$-18 \le h \le 18$, $-14 \le k \le 18$ $-21 \le l \le 21$,
Crystal size (mm)	0.24 × 0.22 × 0.20	0.21 × 0.22 × 0.24	0.15 × 0.17 × 0.21
Reflections collected	21 343/10 337 [$R_{int} = 0.0117$]	16 016/5173 [$R_{int} = 0.050$]	17 095/7925 [$R_{int} = 0.030$]
Independent reflection	10 337	5173	7925
Data/restraints/parameters	10 337/12/642	5173/3/329	7925/45/600
Final R indices [$I > 2\sigma(I)$][a]	$R_1 = 0.0469$, w$R_2 = 0.0959$	$R_1 = 0.0479$, w$R_2 = 0.0888$	$R_1 = 0.0365$, w$R_2 = 0.0760$
R indices (all data)[b]	$R_1 = 0.0645$, w$R_2 = 0.0986$	$R_1 = 0.082$, w$R_2 = 0.1022$	$R_1 = 0.0546$, w$R_2 = 0.0874$

[a] $R_1 = \sum||F_o| - |F_c||/\sum|F_o|$. [b] $wR_2 = [\sum w(F_o^2 - F_c^2)^2/\sum w(F_o^2)^2]^{1/2}$, $w = [\sigma^2(F_o^2) + (0.0784P)^2 + 1.3233P]^{-1}$, where $P = (F_o^2 + 2F_c^2)/3$.

Complex **1**, dark green crystals, yields 12.57 mg, 48.37%. Elemental analysis: anal. calc. for $C_{44}H_{56}Cl_6CaN_4O_{18}Ni_2$ (%): C 40.68; H 4.34; N 4.31; Ni 9.04; Ca 3.09. Found (%): C 40.25; H 4.31; N 4.62; Ni 8.98; Ca 3.01. IR (KBr; cm^{-1}): 1599 [ν(C=N)], 1231 [ν(Ar–O)], 3413 [ν(O–H)]. UV-vis [in methanol/dichloromethane (1 : 1)], λ_{max} (nm) [2.5 × 10^{-5} M]: 284, 370.

Complex **2**, dark green crystals, yields 11.14 mg, 44.65%. Elemental analysis: anal. calc. for $C_{42}H_{54}Cl_4SrN_4O_{18}Ni_2$ (%): C 40.37; H 4.36; N 4.48; Ni 9.39; Sr 7.01. Found (%): C 40.25; H 4.31; N 4.62; Ni 9.26; Sr 6.92. IR (KBr; cm^{-1}): 1597 [ν(C=N)], 1233 [ν(Ar–O)], 3413 [ν(O–H)]. UV-vis [in methanol/dichloromethane (1 : 1)], λ_{max} (nm) [2.5 × 10^{-5} M]: 284, 370.

Complex **3**, dark green crystals, yields 17.26 mg, 38.69%. Elemental analysis: anal. calc. for $C_{78}H_{96}Ba_2N_8O_{36}Ni_4$ (%): C 41.99; H 4.34; N 5.02; Ni 10.52; Ba 12.31. Found (%): C 41.82; H 4.28; N 5.96; Ni 10.47; Ba 12.26. IR (KBr; cm^{-1}): 1593 [ν(C=N)], 1242 [ν(Ar–O)], 3402 [ν(O–H)]. UV-vis [in methanol/dichloromethane (1 : 1)], λ_{max} (nm) [2.5 × 10^{-5} M]: 284, 370.

X-ray crystallographic analysis

The single crystals of complexes **1–3** were placed on a SuperNova, Dual, Cu at zero, Eos four-circle diffractometer. The diffraction data were collected using a graphite monochromated Mo Kα radiation (λ = 0.71073 Å). Reflection data were corrected for Lorentz and polarization factor sand for absorption using the multi-scan method.[16] The structures were solved by using the program SHELXL-2016 and Fourier difference techniques, and refined by the full-matrix least-squares method on F^2. Anisotropic thermal parameters were used for the nonhydrogen atoms and isotropic parameters for the hydrogen atoms. Hydrogen atoms were added geometrically and refined using a riding model. The crystallographic data are summarized in Table 1. CCDC – 1562392 (**1**), 1562393 (**2**) and 1562394 (**3**)† contain the supplementary crystallographic data for this paper.

Results and discussion

The ligand H_4L and its corresponding metal complexes **1–3** are stable in air. The ligand H_4L is remarkably soluble in DMF and DMSO, but slightly soluble in ethyl acetate, acetone, acetonitrile, methanol and ethanol. Complexes **1–3** are absolutely soluble in DMF and DMSO, but slightly soluble in chloroform, dichloromethane, methanol and ethanol at room temperature.

In the ^{1}H NMR spectrum of H_4L, the peaks of methylene protons were observed *ca.* at 4.58 ppm, and the peaks of oxime protons were observed at 8.29 and 9.14 ppm. The OH resonances at 9.82 and 11.03 ppm strongly, respectively, showing the symmetrical structure of H_4L (Fig. S1†). In the ^{13}C NMR spectrum of H_4L, the peaks of the C=N carbon atoms were observed at 148.2 and 148.4 ppm, and the signals of CH_3 carbon atoms were observed at 56.31 ppm (Fig. S2†).

IR spectra analyses

IR spectra of H_4L and its corresponding Ni(II)–M(II) complexes **1–3** exhibit various bands in the region of 4000–400 cm^{-1}

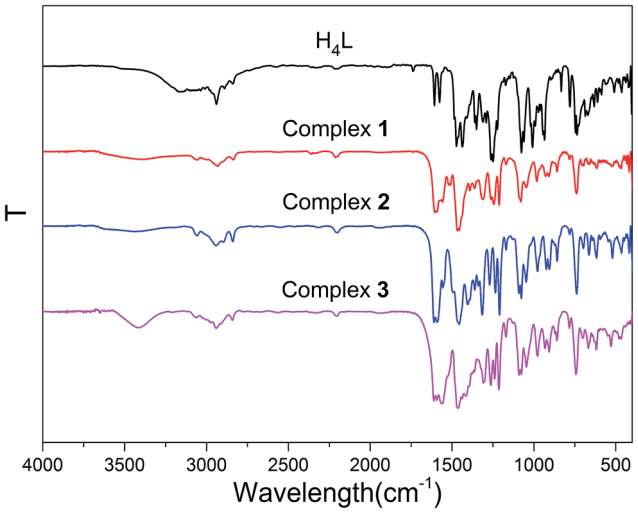

Fig. 1 IR spectra of the ligand H_4L and its corresponding complexes **1–3**.

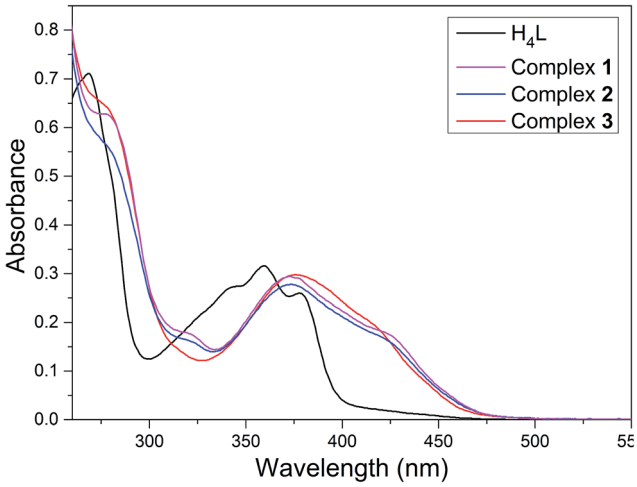

Fig. 2 UV-vis spectra of the ligand H_4L and its corresponding complexes **1–3** in methanol/dichloromethane (1 : 1) ($c = 2.5 \times 10^{-5}$ M).

(Fig. 1). The O–H stretching band of the free ligand H_4L has been observed at *ca.* 3172 cm^{-1} that belongs to the phenolic hydroxyl group, whereas complex **1**, **2** and **3** shows a band at *ca.* 3413, 3413 and 3402 cm^{-1} that belongs to coordinated methanol molecules.[17]

The free ligand H_4L exhibits characteristic C=N stretching band at *ca.* 1604 cm^{-1}, which is shifted by *ca.* 5, 7, 11 cm^{-1} in complexes **1**, **2** and **3**, respectively, indicating that the nitrogen atoms of C=N group are coordinated to the Ni(II) atoms,[18] which is similar to previously reported Ni(II) complexes.[19]

The Ar–O stretching frequency appears at *ca.* 1248 cm^{-1} for the ligand H_4L, while the Ar–O stretching frequencies in complexes **1**, **2** and **3** are observed at *ca.* 1231, 1233 and 1242 cm^{-1}, respectively. The Ar–O stretching frequencies are shifted to lower frequencies, indicating that the M–O bonds are formed between the metal(II) atoms and oxygen atoms of phenolic groups.[20]

UV-vis spectra analyses and fluorescence properties

The methanol/dichloromethane (1 : 1) solutions of the ligand H_4L and its heterometallic Ni(II)–M(II) complexes show, as expected, almost identical UV-vis spectra (Fig. 2).

The free ligand H_4L shows four absorption peaks at 267, 341, 356 and 376 nm. The absorption peak at 267 nm can be assigned to the π–π* transition of the benzene rings and the other bands at 341, 356 and 376 nm can be attributed to the intra-ligand n–π* transition of the C=N bonds and conjugated aromatic chromophore.[21] Compared to the absorption peaks of the free ligand H_4L, with the emergence of two absorption peaks at *ca.* 284 and 370 nm are observed in complexes **1–3**, which can be assigned to π–π* type transition (MLCT). The absorption peaks of complexes **1–3** are bathochromically shifted,[22] indicating coordination of $(L)^{4-}$ ligand unit. The coordination of metal atoms to the binding sites of N_2O_2 and hydroxyl oxygen of the naphthalene ring breaks the intramolecular hydrogen-bonding interactions of H_4L and increases the coplanarity of the conjugated system which causes changes in the UV-vis spectra.[23]

The fluorescent properties of H_4L was determined in DMF solution (2.5×10^{-5} mol L^{-1}) by addition of $Ni(OAc)_2 \cdot 4H_2O$, $Ca(OAc)_2$, $Sr(OAc)_2$ and $Ba(OAc)_2$ in methanol/H_2O (1 : 1) solution (1×10^{-3} mol L^{-1}) are shown in Fig. 3.

The excitation wavelengths of these complexes were measured several times by using the maximum absorption wavelengths, which is the UV-vis spectral theoretical excitation wavelength. The optimal excitation wavelength of these complexes at 378 nm with the maximum emission wavelength is 437 nm.

The fluorescence titration experiment were measured by the addition of Ni^{2+} is shown in Fig. 3(a), the free ligand H_4L shows remarkable fluorescence quenching with maximum emission at *ca.* 437 nm upon the addition of Ni^{2+}. When the added amount of the Ni^{2+} reached 3.0 equiv., the fluorescence emission intensity almost complete quenching and became stable. Weakened of fluorescence is possible due to the coordination of metal ion with the ligand.[24] The spectroscopic titration indicated that the stoichiometric ratio between Ni^{2+} and ligand unit $(L)^{4-}$ was 3 : 1, which signify the Ni(II) complex was formed.[6c,18b] Then, Ca^{2+}, Sr^{2+} and Ba^{2+} were added to the Ni(II) complex, respectively. As shown in Fig. 3(b)–(d), the fluorescence intensity gradually increased, when the added amount of the Ca^{2+} reached 1.0 equiv., the fluorescence intensity reached the maximum, which because one Ni^{2+} in the Ni(II) complex was replaced by one Ca^{2+}, Sr^{2+} or Ba^{2+}, respectively.[6c,18b] This phenomenon may be due to the difference between the radius of the Ni^{2+} and the alkaline earth metal ion.

Titration of Ni(II) complex with Ca^{2+}, Sr^{2+} or Ba^{2+} were followed by fluorescence spectroscopy to determine the binding constant, respectively. As shown in Fig. S4,† the binding constant K of Ni(II) complex with Ca^{2+}, Sr^{2+} and Ba^{2+} were estimated to be 8.14×10^3 M^{-1}, 3.01×10^3 M^{-1} and 8.82×10^2 M^{-1} by the Benesi–Hildebrand equation (fluorescence method) way, respectively,[25] which unambiguously demonstrates stronger binding ability of Ni(II) complex with Ca^{2+}.

According to the obtained experimental data, the differences among the three heterometallic complexes are very obvious and could be utilized in host–guest systems.

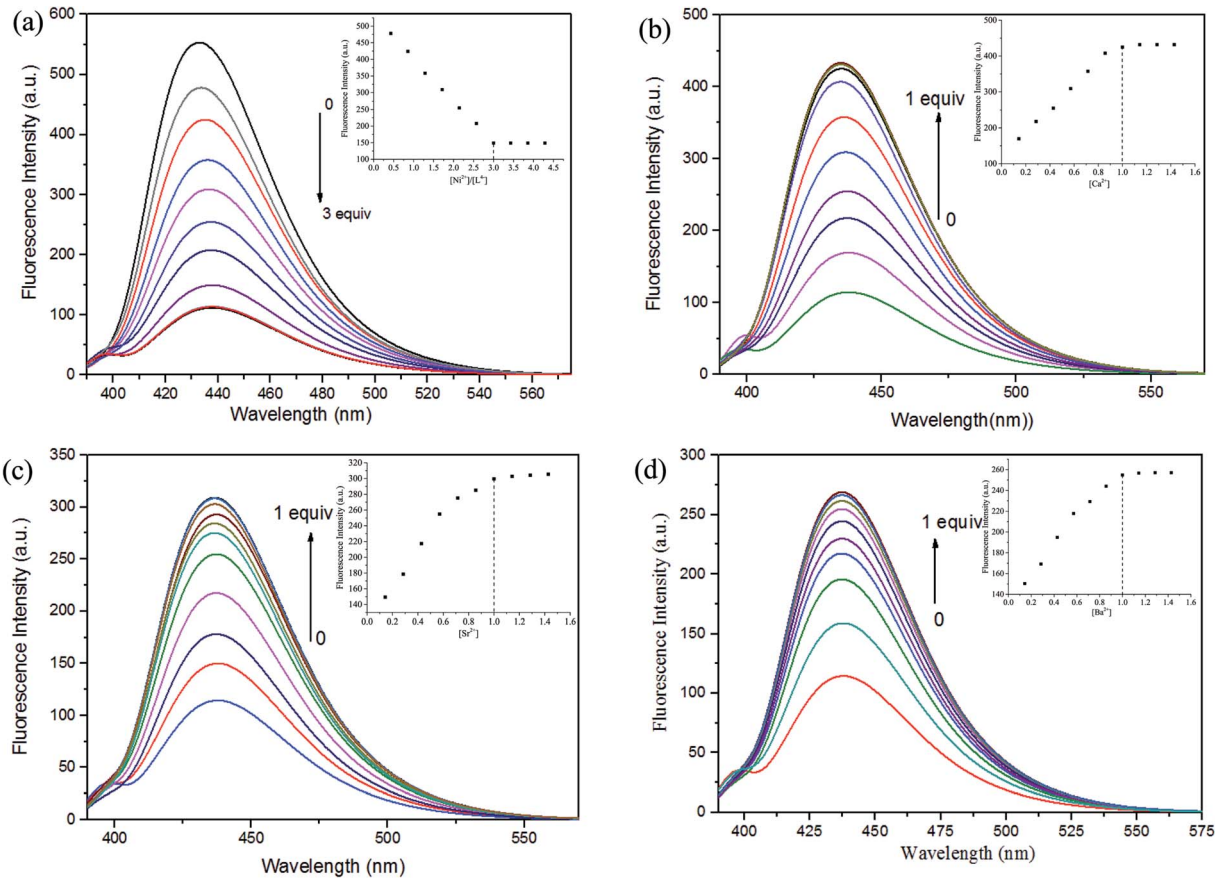

Fig. 3 (a) Absorption spectra of H_4L in DMF solution upon the addition of Ni^{2+}. (b) Absorption spectra of the Ni(II) complex in DMF solution upon the addition of Ca^{2+}. (c) Absorption spectra of the Ni(II) complex in DMF solution upon the addition of Sr^{2+}. (d) Absorption spectra of the Ni(II) complex in DMF solution upon the addition of Ba^{2+}.

Description of the crystal structures

The crystal structures of the heterometallic complexes **1–3** were determined by single-crystal X-ray diffraction. Selected bond lengths and angles of complexes **1–3** are listed in Table 2.

Crystal structure of complexes 1 and 2

The crystal structures and atom numberings of complexes **1** and **2** are shown in Fig. 4 and 5, respectively. X-ray crystallographic analysis of complex **1** reveals a trinuclear structure. It crystallizes in the monoclinic system, space group $P2_1/n$, and consists of two Ni(II) atoms, one Ca(II) atom, one $(L)^{4-}$ unit, two μ_2-acetate ions, two coordinated methanol molecules and two crystallized ethanol and chloroform molecules. While complex **2** crystallizes in the orthorhombic crystal system, space group *Pbcn*, and consists of two Ni(II) atoms, one Sr(II) atom, one $(L)^{4-}$ unit, two μ_2-acetate ions, two coordinated methanol molecules and two crystallized methanol and dichloromethane molecules. X-ray crystallography clearly shows the formation of complexes **1** and **2**, which was isolated as dark green crystals.

Interestingly, the formation process of complex **1** was highly cooperative. In the crystal structure of complex **1**, the terminal Ni(II) atom (Ni1 or Ni2) is located in the N_2O_2 coordination cavity of completely deprotonated $(L)^{4-}$ unit, one oxygen atom (O14 or O11) from the μ_2-acetate bridge and one oxygen atom (O15 or O16) from the coordinated methanol molecule. Because of Ni1 and Ni2 are symmetry related, they have identical geometries. Thus, the Ni1 and Ni2 atoms are both hexa-coordinated with slightly distorted octahedral geometries.[26] While the central Ca1 atom is located in the O_6 cavity, the four are phenoxy oxygen atoms (O2, O5, O6 and O9) while two others (O1 and O10) come from methoxy groups. Besides, two μ_2-acetate ions bridge the two terminal Ni(II) atoms and the central Ca(II) atom in a μ_2-fashion. So the Ca1 atom is octa-coordinated with a slightly distorted square antiprism geometry. The Ca1 atom of complex **1** has strong coordination with the four phenoxy oxygen atoms (O2, O5, O6 and O9) of the $(L)^{4-}$ units and the two oxygen atoms (O12 and O13) of the μ_2-acetate ions by analyzing the distances of the eight Ca1–O bonds. The distances between the Ca1 atom and the four phenoxy oxygen atoms (O2, O5, O6 and O9) and the two μ_2-acetate oxygen atoms (O12 and O13) are ranged from 2.386(2) to 2.409(2) Å, which are obviously shorter than the distances of the other two Ca1–O bonds (Ca1–O1 2.609(2) Å and Ca1–O10 2.605(2) Å). The coordination of complex **2** is similar to that of complex **1**. In the crystal structure of complex **2**, the distances between the Sr1 atom and the four phenoxy oxygen atoms (O2, O5, $O2^{\#1}$ and $O5^{\#1}$) and the two μ_2-acetate oxygen atoms (O7 and $O7^{\#1}$) are ranged from 2.511(2) to

Table 2 Selected bond lengths (Å) and angles (°) of complexes **1**, **2** and **3**[a]

Complex 1					
Ni1–O2	2.020(2)	Ni1–O5	1.963(2)	Ni1–O14	2.079(2)
Ni1–O15	2.196(2)	Ni1–N1	2.071(3)	Ni1–N2	2.062(2)
Ni2–O6	1.968(2)	Ni2–O9	2.018(2)	Ni2–O11	2.082(2)
Ni2–O16	2.179(2)	Ni2–N3	2.066(3)	Ni2–N4	2.055(3)
Ca1–O1	2.609(2)	Ca1–O2	2.405(2)	Ca1–O5	2.386(2)
Ca1–O6	2.404(2)	Ca1–O9	2.404(2)	Ca1–O10	2.605(2)
Ca1–O12	2.393(2)	Ca1–O13	2.409(2)		
O2–Ni1–O5	83.63(9)	O2–Ni1–O14	91.39(9)	O2–Ni1–O15	88.79(9)
O2–Ni1–N1	86.59(10)	O2–Ni1–N2	169.72(10)	O5–Ni1–O14	91.05(9)
O5–Ni1–O15	85.37(9)	O5–Ni1–N1	167.96(11)	O5–Ni1–N2	88.15(10)
O14–Ni1–O15	176.37(9)	O14–Ni1–N1	96.21(10)	O14–Ni1–N2	94.94(11)
O15–Ni1–N1	87.42(10)	O15–Ni1–N2	84.38(10)	N1–Ni1–N2	100.74(11)
O6–Ni2–O9	83.04(8)	O6–Ni2–O11	92.06(9)	O6–Ni2–O16	85.99(9)
O6–Ni2–N3	88.35(10)	O6–Ni2–N4	168.08(11)	O9–Ni2–O11	92.18(9)
O9–Ni2–O16	88.79(9)	O9–Ni2–N3	169.62(10)	O9–Ni2–N4	87.27(10)
O11–Ni2–O16	177.70(8)	O11–Ni2–N3	93.92(10)	O11–Ni2–N4	95.25(10)
O16–Ni2–N3	84.83(10)	O16–Ni2–N4	86.88(10)	N3–Ni2–N4	100.51(11)
O1–Ca1–O2	61.28(7)	O1–Ca1–O5	120.48(8)	O1–Ca1–O6	152.21(8)
O1–Ca1–O9	102.73(7)	O1–Ca1–O10	69.83(7)	O1–Ca1–O12	76.33(8)
O1–Ca1–O13	117.57(8)	O2–Ca1–O5	67.31(7)	O2–Ca1–O6	131.84(7)
O2–Ca1–O9	161.47(8)	O2–Ca1–O10	102.24(7)	O2–Ca1–O12	105.29(8)
O2–Ca1–O13	77.80(8)	O5–Ca1–O6	64.54(7)	O5–Ca1–O9	131.22(8)
O5–Ca1–O10	151.85(8)	O5–Ca1–O12	90.77(8)	O5–Ca1–O13	76.17(8)
O6–Ca1–O9	66.68(7)	O6–Ca1–O10	119.98(8)	O6–Ca1–O12	76.28(8)
O6–Ca1–O13	90.21(8)	O9–Ca1–O10	61.33(7)	O9–Ca1–O12	77.73(8)
O9–Ca1–O13	104.34(8)	O10–Ca1–O12	117.38(8)	O10–Ca1–O13	76.06(8)
O12–Ca1–O13	164.39(8)				
Complex 2					
Ni1–O2	2.011(3)	Ni1–O5	1.984(2)	Ni1–O6	2.063(3)
Ni1–O8	2.169(3)	Ni1–N1	2.068(3)	Ni1–N2	2.042(3)
Sr1–O1	2.667(3)	Sr1–O2	2.517(2)	Sr1–O5	2.511(2)
Sr1–O7	2.525(3)	Sr1–O1$^{\#1}$	2.667(3)	Sr1–O2$^{\#1}$	2.517(2)
Sr1–O5$^{\#1}$	2.511(2)	Sr1–O7$^{\#1}$	2.525(3)		
O2–Ni1–O5	86.26(10)	O2–Ni1–O6	91.73(10)	O2–Ni1–O8	87.13(10)
O2–Ni1–N1	86.72(12)	O2–Ni1–N2	170.41(12)	O5–Ni1–O6	92.21(10)
O5–Ni1–O8	86.08(11)	O5–Ni1–N1	170.72(12)	O5–Ni1–N2	86.94(12)
O6–Ni1–O8	178.00(10)	O6–Ni1–N1	94.07(12)	O6–Ni1–N2	95.27(12)
O8–Ni1–N1	87.51(12)	O8–Ni1–N2	85.68(12)	N1–Ni1–N2	99.27(14)
O1–Sr1–O2	60.20(8)	O1–Sr1–O5	118.79(8)	O1–Sr1–O7	116.48(9)
O1–Sr1–O1$^{\#1}$	76.99(1)	O1–Sr1–O2$^{\#1}$	108.97(8)	O1–Sr1–O5$^{\#1}$	150.00(8)
O1–Sr1–O7$^{\#1}$	76.83(9)	O2–Sr1–O5	65.81(8)	O2–Sr1–O7	75.92(8)
O2–Sr1–O1$^{\#1}$	108.97(8)	O2–Sr1–O2$^{\#1}$	167.40(8)	O2–Sr1–O5$^{\#1}$	126.78(8)
O2–Sr1–O7$^{\#1}$	105.89(8)	O5–Sr1–O7	73.26(9)	O5–Sr1–O1$^{\#1}$	150.00(8)
O5–Sr1–O2$^{\#1}$	126.78(8)	O5–Sr1–O5$^{\#1}$	61.16(8)	O5–Sr1–O7$^{\#1}$	92.77(9)
O7–Sr1–O1$^{\#1}$	76.83(9)	O7–Sr1–O2$^{\#1}$	105.89(8)	O7–Sr1–O5$^{\#1}$	92.76(9)
O7–Sr1–O7$^{\#1}$	163.99(10)	O1$^{\#1}$–Sr1–O2$^{\#1}$	60.21(8)	O1$^{\#1}$–Sr1–O5$^{\#1}$	118.79(8)
O1$^{\#1}$–Sr1–O7$^{\#1}$	116.49(9)	O2$^{\#1}$–Sr1–O5$^{\#1}$	65.81(8)	O2$^{\#1}$–Sr1–O7$^{\#1}$	75.93(8)
O5$^{\#1}$–Sr1–O7$^{\#1}$	73.27(9)				
Complex 3					
Ni2–O5	2.085(3)	Ni2–O8	2.006(3)	Ni2–O20	2.017(3)
Ni2–O22	2.14(6)	Ni2–N14	2.077(3)	Ni2–N18	2.033(3)
Ni3–O9	2.005(3)	Ni3–O12	2.152(3)	Ni3–O13	2.045(3)
Ni3–O16	2.059(3)	Ni3–N25	2.052(3)	Ni3–N35	2.090(3)
Ba1–O8	2.699(3)	Ba1–O9	2.683(3)	Ba1–O11	2.788(3)
Ba1–O13	2.695(3)	Ba1–O17	2.897(3)	Ba1–O19	2.858(3)
Ba1–O20	2.696(3)	Ba1–O23	2.761(3)	Ba1–O15$^{\#2}$	3.128(3)
O5–Ni2–O8	88.26(11)	O5–Ni2–O20	91.72(12)	O5–Ni2–O22	177.6(15)
O5–Ni2–N14	90.56(12)	O5–Ni2–N18	91.04(12)	O8–Ni2–O20	85.98(11)
O8–Ni2–O22	90.8(10)	O8–Ni2–N14	173.33(13)	O8–Ni2–N18	86.40(12)
O20–Ni2–O22	86.0(15)	O20–Ni2–N14	87.50(13)	O20–Ni2–N18	171.80(12)
N14–Ni2–O22	90.1(9)	N18–Ni2–O22	91.1(14)	N14–Ni2–N18	100.19(14)
O9–Ni3–O12	84.24(11)	O9–Ni3–O13	91.41(11)	O9–Ni3–O16	89.72(11)

Table 2 (*Contd.*)

O9–Ni3–N25	174.23(13)	O9–Ni3–N35	83.75(12)	O12–Ni3–O13	87.89(12)
O12–Ni3–O16	173.76(11)	O12–Ni3– N25	90.16(13)	O12–Ni3–N35	87.00(12)
O13–Ni3–O16	90.70(12)	O13–Ni3–N25	86.97(13)	O13–Ni3–N35	173.28(11)
O16–Ni3–N25	95.83(13)	O16–Ni3–N35	93.92(13)	N25–Ni3–N35	97.39(14)
O8–Ba1–O9	57.67(7)	O8–Ba1–O11	107.89(8)	O8–Ba1–O13	122.39(8)
O8–Ba1–O17	172.94(8)	O8–Ba1–O19	111.07(8)	O8–Ba1–O20	61.13(8)
O8–Ba1–O23	90.11(9)	O9–Ba1–O11	145.91(8)	O9–Ba1–O13	65.25(8)
O9–Ba1–O17	121.39(8)	O9–Ba1–O19	135.21(8)	O9–Ba1–O20	115.47(8)
O9–Ba1–O23	65.68(9)	O11–Ba1–O13	115.18(9)	O11–Ba1–O17	68.85(8)
O11–Ba1–O19	77.65(9)	O11–Ba1–O20	71.30(9)	O11–Ba1–O23	148.41(9)
O13–Ba1–O17	56.15(8)	O13–Ba1–O19	113.98(9)	O13–Ba1–O20	168.29(8)
O13–Ba1–O23	72.47(9)	O17–Ba1–O19	74.75(9)	O17–Ba1–O20	121.90(8)
O17–Ba1–O23	95.67(9)	O19–Ba1–O20	56.57(8)	O19–Ba1–O23	71.61(9)
O20–Ba1–O23	96.91(9)				

[a] Symmetry transformations used to generate equivalent atoms: $^{\#1}$ $-x+1, -y+1, -z+1$ (complex **2**); $^{\#2}$ $-x+1, y, -z+3/2$ (complex **3**).

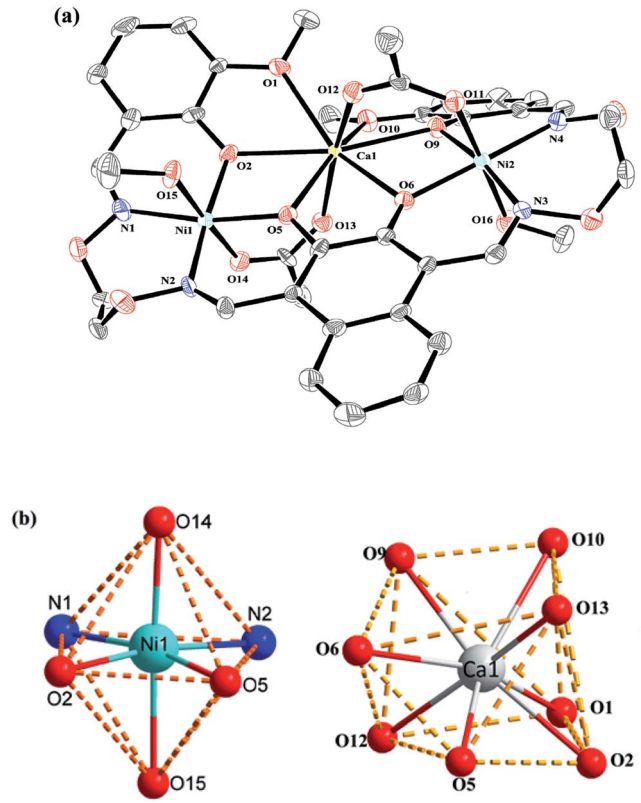

Fig. 4 (a) View of the molecular structure of complex **1** (hydrogen atoms and solvent molecules are omitted for clarity, and thermal ellipsoids are drawn at the 30% probability level). (b) Coordination polyhedra for Ni(II) and Ca(II) atoms of complex **1**.

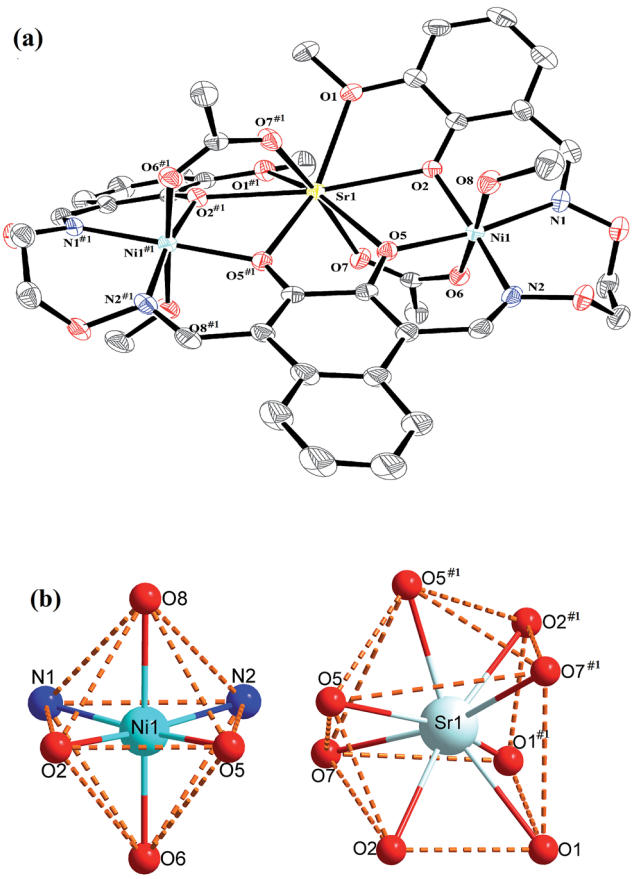

Fig. 5 (a) View of the molecular structure of complex **2** (hydrogen atoms and solvent molecules are omitted for clarity, and thermal ellipsoids are drawn at the 30% probability level). (b) Coordination polyhedra for Ni(II) and Sr(II) atoms of complex **2**.

2.525(3) Å, which are obviously shorter than the distances of the other two Sr1–O bonds (Sr1–O1 2.667(3) Å and Sr1–O1$^{\#1}$ 2.667(3) Å). Obviously, the Sr–O bond lengths in complex **2** are larger than the corresponding Ca–O bond lengths found in complex **1**.

Crystal structure of complex 3

The crystal structure and atom numbering of complex **3** is shown in Fig. 6. Complex **3** crystallizes in the monoclinic crystal system, space group $P2_1/n$. In complex **3**, the terminal Ni(II) atom (Ni2 or Ni3) is hexa-coordinated with a slightly distorted octahedral geometry. Where the inner N_2O_2 cavities of completely deprotonated $(L)^{4-}$ units as the basal plane, and one oxygen atom (O22) from the coordinated methanol molecule, the other oxygen atom (O5) from the coordinated H_2O molecule

for the Ni2 atom. Similarly, one oxygen atom (O12) from the coordinated methanol molecule, the other oxygen atom (O16) from the μ-acetate ion for the Ni3 atom. It is unexpected that the coordination of two μ_2-acetate ions bridge the Ba1 and Ba1$^{\#2}$ atoms in a familiar μ_2-fashion, finally forming a hetero-hexanuclear dimer. To our knowledge, this novel 2 : 6 ($(L)^{4-}$: M^{2+}) heterohexanuclear complex isn't reported in the bis(salamo)-type complexes.[1,2e,11c]

The central Ba1 atom is nona-coordinated with a slightly distorted tricapped trigonal prism geometry, which is different from the Ca1 and Sr1 atoms. The distances between the Ba1 atom and the four phenoxy oxygen atoms (O8, O9, O13 and O20) and the μ_2-acetate oxygen atom (O23) are ranged from 2.683(3) to 2.761(3) Å, which are evidently shorter than the distances between the Ba1 atom and the two methoxy oxygen atoms (O17 and O19) (Ba1–O17 2.897(3) Å and Ba1–O19 2.858(3) Å) and the two μ_2-acetate oxygen atoms (O11 and O15$^{\#2}$) (Ba1–O11 2.788(3) Å and Ba1–O15$^{\#2}$ 3.128(3) Å).

As a result, when the two N_2O_2 salamo moieties are metalated with d-block transition metals, the conformation of the molecules is restricted so that the phenoxo oxygen atoms are directed inward to form an O_6 cavity. Since the O_6 cavity is large, the Ca(II), Sr(II) or Ba(II) atoms are suitable for this size, and will coordinate to form the C-shaped complexes.

The resulting geometries of Ni1 and Ni2 are both distorted octahedral geometries with hexa-coordinated, Ca1 and Sr1 are octa-coordinated with geometries of square antiprisms respectively. However, Ba1 has bigger size than the cavity, so the coordination of metal atoms with the methanol molecules and H_2O makes the structure more stable. The resulting geometry of Ba1 is rarely tricapped trigonal prismatic geometry. As the cation radius increases, the coordination bond lengths of the central cation are distinctly becoming larger and larger. This fact suggests that the radius size of central cation is a significant factor which affects binding ability of the central O_6 site. As a result, the coordinating capability in the central O_6 site is in the order of Ca(II) > Sr(II) > Ba(II), which obtained the same conclusion with fluorescent titration.

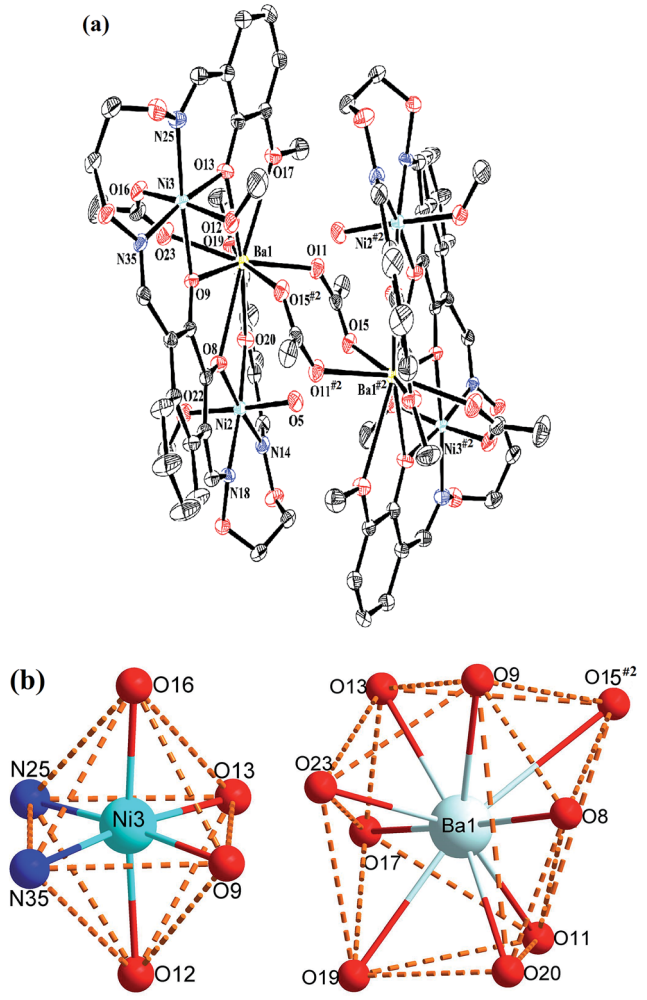

Fig. 6 (a) View of the molecular structure of complex 3 (hydrogen atoms are omitted for clarity, and thermal ellipsoids are drawn at the 30% probability level). (b) Coordination polyhedra for Ni(II) and Ba(II) atoms of complex 3.

Conclusion

Three heterometallic Ni(II)–M(II) (M = Ca, Sr and Ba) complexes **1–3** have been designed and synthesized. X-ray crystal structures reveal that the different nature of the N_2O_2 and O_6 sites of the ligand H_4L leads to the site-selective introduction of two different kinds of metal(II) atoms. The coordination number of Ca(II) Sr(II) and Ba(II) atoms in the O_6 environment are 8, 8 and 9, respectively, and have slightly square antiprism and square tricapped trigonal prism gemtries. As a result, the coordinating capability in the central O_6 site is in the order of Ca(II) > Sr(II) > Ba(II). Fluorescence titration experiments show that Ni^{2+} led to the fluorescence quenching of H_4L. Owing to their electrostatic interaction and their size-fit principle, rare-earth(III) atoms would easier to occupy the center of the O_6 position successfully, which could be used for the recognition of rare-earth(III) atoms. The related research is underway.

Conflicts of interest

There are no conflicts to declare.

Acknowledgements

This work was supported by the National Natural Science Foundation of China (21361015 and 21761018) and the Program for Excellent Team of Scientific Research in Lanzhou Jiaotong University (201706), which are gratefully acknowledged.

References

1 S. Akine, T. Taniguchi and T. Nabeshima, *Inorg. Chem.*, 2008, **47**, 3255–3264.
2 (*a*) G. Murugavel, P. Sadhu and T. Punniyamurthy, *Chem. Rec.*, 2016, **16**, 1906–1917; (*b*) Y. Xu, D. Yuan, Y. Wang and Y. Yao, *Dalton Trans.*, 2017, **46**, 5848–5855; (*c*) H. L. Wu, Y. C. Bai, Y. H. Zhang, G. L. Pan, J. Kong, F. R. Shi and X. L. Wang, *Z. Anorg. Allg. Chem.*, 2014, **640**, 2062–2071; (*d*)

X. Q. Song, P. P. Liu, Z. R. Xiao, X. Li and Y. A. Liu, *Inorg. Chim. Acta*, 2015, **438**, 232–244; (*e*) L. Chen, W. K. Dong, H. Zhang, Y. Zhang and Y. X. Sun, *Cryst. Growth Des.*, 2017, **17**, 3636–3648; (*f*) X. Y. Li, L. Chen, L. Gao, Y. Zhang, S. F. Akogun and W. K. Dong, *RSC Adv.*, 2017, **7**, 35905–35916; (*g*) E. V. Alekseeva, I. A. Chepurnaya, V. V. Malev, A. M. Timonovb and O. V. Levina, *Electrochim. Acta*, 2017, **225**, 378–391; (*h*) R. Irie and T. Katsuki, *Chem. Rec.*, 2004, **4**, 96–109; (*i*) T. Nabeshima and S. Akine, *Chem. Rec.*, 2008, **8**, 240–251.

3 (*a*) P. P. Liu, L. Sheng, X. Q. Song, W. Y. Xu and Y. A. Liu, *Inorg. Chim. Acta*, 2015, **434**, 252–257; (*b*) X. Q. Song, Y. Q. Peng, G. Q. Cheng, X. R. Wang, P. P. Liu and W. Y. Xu, *Inorg. Chim. Acta*, 2015, **427**, 13–21.

4 (*a*) X. Y. Dong, Y. X. Sun, L. Wang and L. Li, *J. Chem. Res.*, 2012, **36**, 387–390; (*b*) P. Wang and L. Zhao, *Spectrochim. Acta, Part A*, 2015, **135**, 342–350; (*c*) C. Y. Chen, J. W. Zhang, Y. H. Zhang, Z. H. Yang, H. L. Wu, G. L. Pan and Y. C. Bai, *J. Coord. Chem.*, 2015, **68**, 1054–1071.

5 (*a*) L. H. Li, W. K. Dong, Y. Zhang, S. F. Akogun and L. Xu, *Appl. Organomet. Chem.*, 2017, DOI: 10.1002/aoc.3818; (*b*) T. K. Chin, S. Endud, S. Jamil, S. Budagumpi and H. O. Lintang, *Catal. Lett.*, 2013, **143**, 282–288.

6 (*a*) W. K. Dong, X. L. Li, L. Wang, Y. Zhang and Y. J. Dong, *Spectrochim. Acta, Part B*, 2016, **229**, 370–378; (*b*) W. K. Dong, S. F. Akogun, Y. Zhang, Y. X. Sun and X. Y. Dong, *Spectrochim. Acta, Part B*, 2017, **238**, 723–734; (*c*) B. J. Wang, W. K. Dong, Y. Zhang and S. F. Akogun, *Spectrochim. Acta, Part B*, 2017, **247**, 254–264.

7 (*a*) W. K. Dong, J. C. Ma, L. C. Zhu, Y. Zhang and X. L. Li, *Inorg. Chim. Acta*, 2016, **445**, 140–148; (*b*) Ş. Ömer, Ö. Ö. Ümmühan, S. Nurgul, A. Burcu, S. Musa, T. Tuncay and S. Zeynel, *Tetrahedron*, 2016, **72**, 5843–5852.

8 (*a*) T. Z. Yu, K. Zhang, Y. L. Zhao, C. H. Yang, H. Zhang, L. Qian, D. W. Fan, W. K. Dong, L. L. Chen and Y. Q. Qiu, *Inorg. Chim. Acta*, 2008, **361**, 233–240; (*b*) Y. J. Dong, X. Y. Dong, W. K. Dong, Y. Zhang and L. S. Zhang, *Polyhedron*, 2017, **123**, 305–315; (*c*) W. K. Dong, J. C. Ma, Y. J. Dong, L. Zhao, L. C. Zhu, Y. X. Sun and Y. Zhang, *J. Coord. Chem.*, 2016, **69**, 3231–3241; (*d*) H. L. Wu, C. P. Wang, F. Wang, H. P. Peng, H. Zhang and Y. C. Bai, *J. Chin. Chem. Soc.*, 2015, **62**, 1028–1034; (*e*) W. K. Dong, J. C. Ma, L. C. Zhu, Y. X. Sun, S. F. Akogun and Y. Zhang, *Cryst. Growth Des.*, 2016, **16**, 6903–6914; (*f*) L. Liu, W. Feng, X. Lu and W. K. Wong, *Inorg. Chem. Commun.*, 2017, **75**, 29–32; (*g*) X. Yang and R. A. Jones, *J. Am. Chem. Soc.*, 2005, **127**, 7686–7687; (*h*) F. Wang, L. Gao, Q. Zhao, Y. Zhang, W. K. Dong and Y. J. Ding, *Spectrochim. Acta, Part A*, 2018, **190**, 111–115.

9 (*a*) W. K. Dong, J. C. Ma, Y. J. Dong, L. C. Zhu and Y. Zhang, *Polyhedron*, 2016, **115**, 228–235; (*b*) S. S. Zheng, W. K. Dong, Y. Zhang, L. Chen and Y. J. Ding, *New J. Chem.*, 2017, **41**, 4966–4973; (*c*) H. Zhang, W. K. Dong, Y. Zhang and S. F. Akogun, *Polyhedron*, 2017, **133**, 279–293; (*d*) P. Seth, S. Ghosh, A. Figuerola and A. Ghosh, *Dalton Trans.*, 2014, **43**, 990–998; (*e*) A. B. Canaj, M. Siczek, M. Otręba, T. Lis, G. Lorusso, M. Evangelisti and C. J. Milioset, *Dalton Trans.*, 2016, **45**, 18591–18602.

10 (*a*) X. Y. Dong, S. F. Akogun, W. M. Zhou and W. K. Dong, *J. Chin. Chem. Soc.*, 2017, **64**, 412–419; (*b*) Y. J. Dong, X. L. Li, Y. Zhang and W. K. Dong, *Supramol. Chem.*, 2017, **29**, 518–527; (*c*) W. K. Dong, J. Zhang, Y. Zhang and N. Li, *Inorg. Chim. Acta*, 2016, **444**, 95–102; (*d*) W. K. Dong, F. Zhang, N. Li, L. Xu, Y. Zhang, J. Zhang and L. C. Zhu, *Z. Anorg. Allg. Chem.*, 2016, **642**, 532–538; (*e*) W. K. Dong, G. Li, Z. K. Wang and D. X. Yong, *Spectrochim. Acta, Part A*, 2014, **133**, 340–347.

11 (*a*) S. Akine, T. Tadokoro and T. Nabeshima, *Inorg. Chem.*, 2012, **51**, 11478–11486; (*b*) S. Akine and T. Nabeshima, *Dalton Trans.*, 2009, **47**, 10395–10408; (*c*) J. Hao, L. L. Li, J. T. Zhang, S. F. Akogun, L. Wang and W. K. Dong, *Polyhedron*, 2017, **134**, 1–10.

12 (*a*) L. Wang, J. C. Ma, W. K. Dong, L. C. Zhu and Y. Zhang, *Z. Anorg. Allg. Chem.*, 2016, **642**, 834–839; (*b*) H. L. Wu, G. L. Pan, H. Wang, X. L. Wang, Y. C. Bai and Y. H. Zhang, *J. Photochem. Photobiol., B*, 2014, **135**, 33–43; (*c*) Y. A. Liu, C. Y. Wang, M. Zhang and X. Q. Song, *Polyhedron*, 2017, **127**, 278–286; (*d*) H. L. Wu, G. L. Pan, Y. C. Bai, H. Wang, J. Kong, F. Shi, Y. H. Zhang and X. L. Wang, *J. Chem. Res.*, 2014, **38**, 211–217; (*e*) H. L. Wu, Y. C. Bai, Y. H. Zhang, Z. Li, M. C. Wu, C. Y. Chen and J. W. Zhang, *J. Coord. Chem.*, 2014, **67**, 3054–3066.

13 H. A. Tran, J. Collins and P. E. Georghiou, *New J. Chem.*, 2008, **32**, 1175–1182.

14 D. W. Dixon and R. H. Weiss, *J. Org. Chem.*, 1984, **49**, 4487–4494.

15 S. Akine, T. Taniguchi, W. K. Dong, S. Masubuchi and T. Nabeshima, *J. Org. Chem.*, 2005, **70**, 1704–1711.

16 G. M. Sheldrick, *Acta Crystallogr., Sect. A: Found. Crystallogr.*, 2008, **64**, 112–122.

17 P. P. Liu, C. Y. Wang, M. Zhang and X. Q. Song, *Polyhedron*, 2017, **129**, 133–140.

18 (*a*) W. K. Dong, P. F. Lan, W. M. Zhou and Y. Zhang, *J. Coord. Chem.*, 2016, **69**, 1272–1283; (*b*) W. K. Dong, S. S. Zheng, J. T. Zhang, Y. Zhang and Y. X. Sun, *Spectrochim. Acta, Part A*, 2017, **184**, 141–150.

19 (*a*) X. Y. Dong, Q. P. Kang, B. X. Jin and W. K. Dong, *Z. Naturforsch.*, 2017, **72**, 415–420; (*b*) L. M. Pu, H. T. Long, Y. Zhang, Y. Bai and W. K. Dong, *Polyhedron*, 2017, **128**, 57–67.

20 W. K. Dong, L. C. Zhu, J. C. Ma, Y. X. Sun and Y. Zhang, *Inorg. Chim. Acta*, 2016, **453**, 402–408.

21 S. Akine, T. Taniguchi and T. Nabeshima, *Chem. Lett.*, 2001, **30**, 682–683.

22 W. K. Dong, L. C. Zhu, Y. J. Dong, J. C. Ma and Y. Zhang, *Polyhedron*, 2016, **117**, 148–154.

23 M. Tümer, H. Köksal, M. K. Sener and S. Serin, *Transition Met. Chem.*, 1999, **24**, 414–420.

24 (*a*) L. Q. Chai, G. Wang, Y. X. Sun, W. K. Dong, L. Zhao and X. H. Gao, *J. Coord. Chem.*, 2012, **65**, 1621–1631; (*b*) L. Q. Chai, K. Y. Zhang, L. J. Tang, J. Y. Zhang and H. S. Zhang, *Polyhedron*, 2017, **130**, 100–107; (*c*) L. Q. Chai, L. J. Tang, L. C. Chen and J. J. Huang, *Polyhedron*, 2017,

122, 228–240; (*d*) L. Xu, L. C. Zhu, J. C. Ma, Y. Zhang, J. Zhang and W. K. Dong, *Z. Anorg. Allg. Chem.*, 2015, **641**, 2520–2524; (*e*) L. Q. Chai, J. J. Huang, J. Y. Zhang and Y. X. Li, *J. Coord. Chem.*, 2015, **68**, 1224–1237; (*f*) X. Q. Song, P. P. Liu, Y. A. Liu, J. J. Zhou and X. L. Wang, *Dalton Trans.*, 2016, **45**, 8154–8163.

25 H. A. Benesi and J. H. Hildebrand, *J. Am. Chem. Soc.*, 1949, **71**, 2703–2707.

26 (*a*) W. K. Dong, J. C. Ma, L. C. Zhu and Y. Zhang, *New J. Chem.*, 2016, **40**, 6998–7010; (*b*) W. K. Dong, L. S. Zhang, Y. X. Sun, M. M. Zhao, G. Li and X. Y. Dong, *Spectrochim. Acta, Part A*, 2014, **121**, 324–329.